Northeast- or southwest-dipping subduction in the Cretaceous Caribbean gateway?

Lithos 386–387 (2021) 105998

Contents lists available at ScienceDirect

Lithos

journal homepage: www.elsevier.com/locate/lithos

Research Article

Northeast- or southwest-dipping subduction in the Cretaceous Caribbean gateway?

Alan R. Hastie [a,*], Sophie Cox [b], Andrew C. Kerr [b]

[a] School of GeoSciences, University of Edinburgh, King's Buildings, Edinburgh EH9 3FE, UK
[b] School of Earth and Environmental Sciences, Cardiff University, Main Building, Park Place, Cardiff CF10 3YE, UK

ARTICLE INFO

Article history:
Received 30 July 2020
Received in revised form 11 January 2021
Accepted 15 January 2021
Available online 23 January 2021

Keywords:
Virgin Islands
Greater Antilles
Water Island Formation
Louisenhoj Formation
Tutu Formation
Subduction initiation
Subduction polarity

ABSTRACT

Most of the Caribbean plate, which currently lies between the American continents, represents a mantle plume-derived 8–20 km thick Cretaceous oceanic plateau that was formed in the Pacific region and moved eastwards. The northern islands of the Caribbean are largely made up of a dismembered island arc that was located along the western entrance to the inter-American region (termed the Great Arc of the Caribbean) in the mid-late Cretaceous. Importantly, the timing of Caribbean lithospheric movement into the inter-American region is controversial, with one hypothesis advocating that it happened in the Hauterivian-Albian (132.9–100.5 Ma), and a second hypothesis proposing the Turonian-Campanian (93.9–72.1 Ma). In order to investigate this problem, island arc rocks are studied on St. John, U.S. Virgin Islands, which are Barremian (127 Ma) to Santonian (83.6 Ma) in age. Immobile trace element and Nd–Hf radiogenic isotope ratios demonstrate that the arc rocks are derived from the partial melting of an Atlantic MORB-like mantle source region that has been variably contaminated with slab-derived fluids composed of continental detritus and slow sediment clay components. We argue that the lack of a mantle plume geochemical signature in the rocks supports the idea that the movement of Caribbean lithosphere into the inter-American region occurred in the late Cretaceous (post-Santonian) due to a subduction polarity reversal caused by collision of the Caribbean oceanic plateau with the Great Arc of the Caribbean.

1. Introduction

The Caribbean plate is situated between the much larger North and South American plates and its eastern and western margins are separated from oceanic crust in the Atlantic and Pacific by active subduction zones. The Caribbean is predominantly composed of an 8–20 km thick Cretaceous oceanic plateau (COP) with Cretaceous to Miocene marginal arc sequences (e.g., Edgar et al., 1971; Hastie and Kerr, 2010; Hauff et al., 2000; Leroy and Mauffret, 1996; Neill et al., 2010). The COP was initially formed in the Pacific region (on the Farallon plate), possibly at the Galapagos hotspot (Buchs et al., 2018; Thompson et al., 2003; Torró et al., 2017; Wright and Wyld, 2011). At the same time, a large island arc was located along the western entrance to the inter-American region (termed the Great Arc of the Caribbean) (Burke, 1988).

After the COP was emplaced onto Farallon oceanic crust it was transported to the northeast and both the plateau and Great Arc moved into the inter-American region and developed into a separate plate (the Caribbean plate) (e.g., Boschman et al., 2014; Burke, 1988; Pindell et al., 2011). As the COP and Great Arc were translated eastwards into the inter-American region, the Great Arc fragmented to form the modern islands of Cuba, Jamaica, Hispaniola, Puerto Rico and the Virgin Islands. Additional arc fragments are represented by the submarine Aves Ridge (west of the Lesser Antilles) and the southern islands of Aruba, Curaçao and Bonaire and parts of Trinidad and Tobago (Escuder Viruete et al., 2008; Kerr et al., 1999; Neill et al., 2011, 2014; Pindell et al., 2011; Wright and Wyld, 2011).

The timing of Caribbean lithospheric movement into the inter-American region is controversial. One hypothesis proposes that the Caribbean plate began to be emplaced between the Americas in the Hauterivian-Albian (132.9–100.5 Ma) (Boschman et al., 2014, 2019; Marchesi et al., 2016; Pindell et al., 2011; Pindell and Kennan, 2009; Torró et al., 2016, 2017). The proposed causal mechanism to allow this early emplacement is variable in the literature, but has been linked to an increase in Atlantic seafloor spreading rate that either (1) generated subduction on a pre-existing inter-American transform fault (Pindell et al., 2011) or (2) initiated a polarity reversal on the existing Great Arc (Pindell and Kennan, 2009). It has also been proposed that an arc-arc collision may have caused the reversal at this time (Boschman et al., 2019).

A second hypothesis advocates that in the Turonian-Campanian (93.9–72.1 Ma) the COP collided with the Great Arc of the Caribbean and initiated a subduction reversal whereby northeast-directed

* Corresponding author.
E-mail address: ahastie@ed.ac.uk (A.R. Hastie).

https://doi.org/10.1016/j.lithos.2021.105998

subduction gave way to southwest-directed subduction (Buchs et al., 2018; Burke, 1988; Hastie et al., 2013; Kerr et al., 1999, 2003; Smith et al., 1998; Thompson et al., 2003; Vallejo et al., 2006). Boschman et al. (2014) also states that the collision model has no kinematic problems and is a plausible scenario.

Studying temporal geochemical changes in the igneous rocks of the Great Arc of the Caribbean can help us determine when Caribbean lithosphere moved into the inter-American region and the timing of subduction polarity reversal. In this contribution, we determine the geochemistry of Barremian to Santonian (127–83.6 Ma) island arc rocks on the U.S. Virgin Island of St. John in order to establish when a plume-like mantle signature replaced a depleted mid-ocean ridge basalt (MORB) mantle signature. Our results will help explain when northeast directed subduction tapping a MORB-like proto-Caribbean mantle changed to southwest directed subduction tapping mantle plume-derived asthenosphere beneath the Caribbean oceanic plateau and so can help resolve when the Caribbean plate began to move into the inter-American region.

2. The Great Arc of the Caribbean

The extinct Cretaceous-Miocene Greater Antilles island arc system, located on the northern Caribbean plate boundary, extends from Cuba and Jamaica in the west to the Virgin Islands in the east (Fig. 1a) (Escuder Viruete et al., 2006, 2010; Escuder Viruete and Castillo Carrión, 2016; Hastie, 2009; Jolly et al., 1998a, 1998b; Jolly and Lidiak, 2006; Kerr et al., 2003; Lebron and Perfit, 1993, 1994; Lidiak and Anderson, 2015; Marchesi et al., 2007; Torró et al., 2016). The similar ages and compositions of igneous rocks throughout the Greater Antilles has persuaded many authors that the arc represents a geochemically evolving (e.g., Lidiak and Anderson, 2015), but singular, continuous volcanic island arc that formed on the Proto-Caribbean-Farallon plate boundary and was then tectonically emplaced into the inter-American region from the mid- or upper-Cretaceous (Boschman et al., 2014; Burke, 1988; Duncan and Hargraves, 1984; Hastie et al., 2009; Jolly et al., 2006, 2008; Jolly and Lidiak, 2006; Kerr et al., 1999, 2003; Kesler et al., 2005; Pindell et al., 2006, 2011).

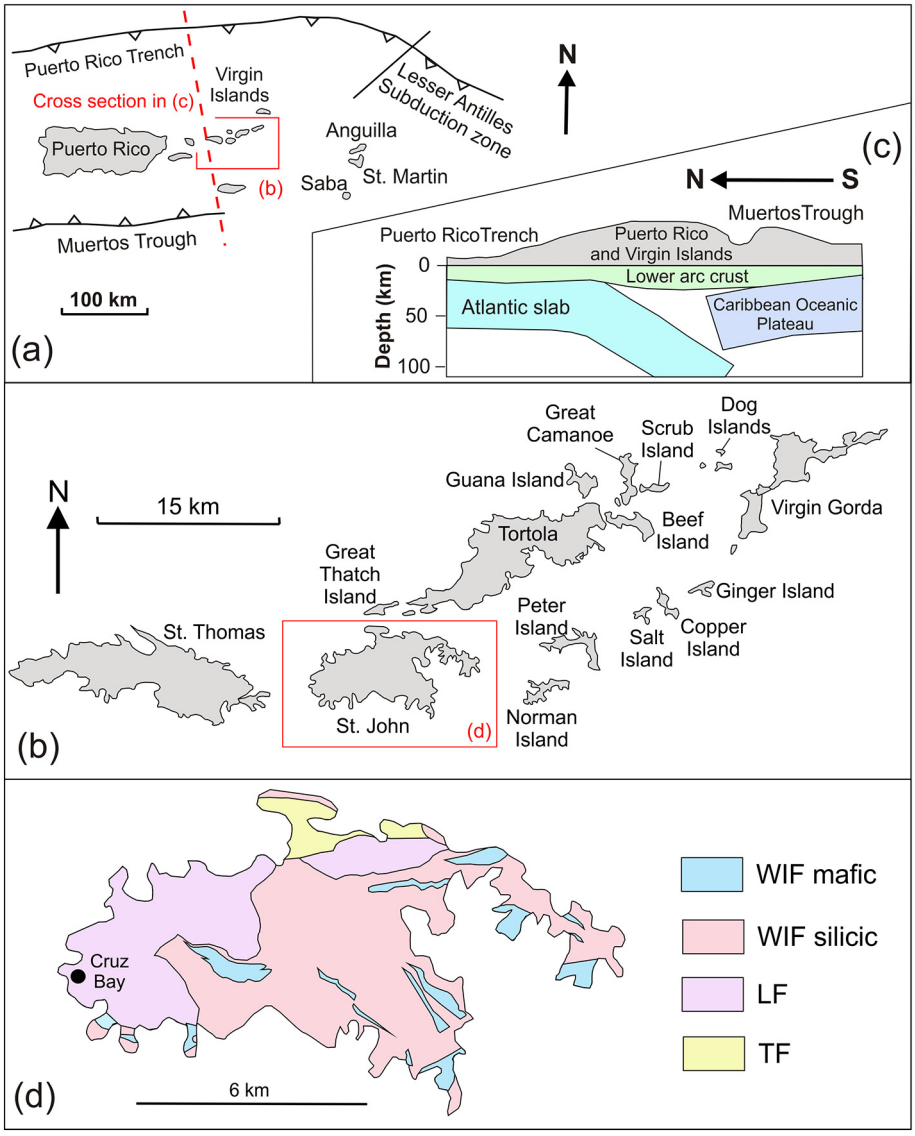

Fig. 1. (a and b) Simplified maps of the northeastern Greater Antilles region and the Virgin Islands archipelago. (c) cross section showing the structure beneath the Puerto Rico and Virgin Islands microplate. Modified from Smith et al. (1998) and Xu et al. (2016). (d) simple geological map of St. John, modified from Rankin (2002). WIF, Water Island Formation; LF, Louisenhoj Formation; TF, Tutu Formation.

The magmatic rocks of the Great Arc are complex in detail (Escuder Viruete and Castillo Carrión, 2016; Torró et al., 2017), but are broadly formed of two compositionally different island arc-derived volcanic rock suites (Hastie, 2009; Jolly et al., 1998a, 1998b, 2006; Lidiak and Anderson, 2015; Marchesi et al., 2007). These two suites were defined by Donnelly et al. (1971) and Donnelly and Rogers (1980) as (1) an island arc tholeiite (IAT) series [termed primitive island arc (PIA) in the older literature] (Jolly et al., 1998b; Kesler et al., 2005; Jolly and Lidiak, 2006; Hastie, 2009) and 2) a calc-alkaline (CA) series that also consists of small volumes of high-K calc-alkaline and shoshonitic rocks (Donnelly et al., 1990; Jolly et al., 1998a, 1998b; Jolly and Lidiak, 2006; Kerr et al., 2003; Lidiak and Anderson, 2015). Recently, boninites have also been discovered in lower Cretaceous successions on the islands of the Great Arc and are frequently found with IAT rocks of the same age (e.g., Escuder Viruete and Castillo Carrión, 2016; Torró et al., 2017). The IAT series is compositionally distinct from the CA series by having lower Th, U, Rb, Ba, K and light rare earth element (LREE) concentrations, throughout the full range of volcanic rock types (basalts to rhyolites) (Donnelly et al., 1990; Donnelly and Rogers, 1980; Frost et al., 1998; Hastie et al., 2009; Jolly et al., 1998a, 1998b, 2006, 2008; Kerr et al., 2003; Lidiak and Anderson, 2015; Marchesi et al., 2007; Schelleckens, 1998). The relative enrichment of large ion lithophile elements (LILE) and LREE in the CA suite has been explained by a range of processes including: (1) lower degrees of partial melting generating incompatible enriched lavas and (2) derivation from a mantle wedge contaminated with a slab-derived fluid containing a variety of sedimentary components (e.g., pelagic vs. terrigenous components) (Escuder Viruete and Castillo Carrión, 2016; Hastie et al., 2009, 2013; Jolly et al., 1998b, 2008; Marchesi et al., 2007; Torró et al., 2017)

3. St. John, U.S. Virgin Islands

The Virgin Islands, the eastern extremity of the Great Arc (Fig. 1a-c), are now located in the northeast corner of the Caribbean plate. Puerto Rico and the Virgin Islands represent a microplate with the Puerto Rico Trench being the current northeast tectonic boundary between the Caribbean plate to the south and the North American plate to the north (Fig. 1a) (Mann et al., 2002;Rankin, 2002; Smith et al., 1998). The three U.S. Virgin Islands of St. Thomas, St. John and St. Croix lie to the southwest of the British Virgin Islands, but all are located where the extinct Greater Antilles arc meets the modern-day active Lesser Antilles to the east (Fig. 1a).

St. John covers an area of ~48 km^2, the stratigraphy was determined by Rankin (2002) and the oldest unit consists of the Barremian-lower Albian (~127–113 Ma) Lameshur Volcanic-Intrusive Complex that is split into the Water Island Formation (WIF) and the Careen Hill Intrusive Suite (e.g., Lidiak and Anderson, 2015; Rankin, 2002; Smith et al., 1998). The Albian-Santonian (113–83.6 Ma) Louisenhoj Formation (LF) and Outer Brass Limestone overlie the WIF and Careen Hill Intrusive Suite, and these are followed conformably by the upper Turonian-upper Santonian (89.8–83.6 Ma) Tutu Formation (TF) (Fig. 1d) (Rankin, 2002; Smith et al., 1998).

The WIF consists of extrusive altered silicic rocks known as keratophyres and related volcaniclastic rocks (~80%), basaltic lavas and breccias (~20%) and minor cherts (Rankin, 2002). The keratophyres are classified by Rankin (2002) into multiple varieties based on the size and mineralogy of the phenocryst populations. The Careen Hill Intrusive Suite is largely composed of intrusive keratophyre (with minor trondhjemite and gabbro) (Rankin, 2002). The plutonic rocks intrude one another and the WIF. The conformably overlying LF is dominantly volcaniclastic, but basaltic, andesitic and keratophyre lavas are found sparsely throughout the formation (Rankin, 2002). The TF is composed of a variety of sedimentary rocks with rare basalts and andesites. Rocks of the Careen Hill Intrusive Suite, WIF, LF and TF have been affected by tropical and hydrothermal alteration and are cut by younger dolerite, gabbro, lamprophyre and tonalite dykes (Rankin, 2002).

4. New petrographic results

4.1. Water Island Formation mafic-intermediate rocks

The basalt and basaltic andesite lavas are porphyritic with <5% sub- to euhedral micro-phenocrysts of plagioclase. Rare clinopyroxene and hornblende phenocrysts up to 3 and 1 mm, respectively, are minor phenocryst constituents. Phenocrysts sit in a commonly aphanitic groundmass of randomly orientated plagioclase needles, (<0.1 mm) with small clinopyroxenes and opaque minerals. Many samples exhibit a randomly orientated groundmass, however, locally plagioclase laths can be aligned and impart a weak foliation to the rock. The basalts have undergone variable alteration and low degree metamorphism with the growth of chlorite, prehnite, pumpellyite and calcite, and in some samples, clinopyroxene is locally replaced by epidote and amphibole (hornblende), and plagioclase to sericite. Amygdales are present as elongated cavities <3 mm-long filled with variable combinations of quartz and epidote with radiating elongate crystals, hornblende, devitrified glass, plagioclase and occasionally, prehnite. Polycrystalline quartz and sericite veins are common and likely formed as secondary features, post-eruption.

4.2. Water Island Formation silicic rocks (includes the Careen Hill Intrusive Suite)

For the remainder of this article, we refer to the evolved rocks in the WIF and CHIS as the WIF because the two rock suites are geochemically identical and the WIF term has been used extensively in previous literature. The WIF keratophyres have been grouped into multiple varieties based on the size and mineralogy of the phenocryst populations by Rankin (2002). A brief summary of the samples used in this study is given below, but for a more detailed classification of the WIF keratophyres the reader is referred to Rankin (2002). Like the basalts, the keratophyres are altered and are predominately porphyritic with phenocrysts of varying size. Typically, all keratophyres have aphanitic groundmasses composed of laths of randomly orientated or aligned albitised plagioclase and interstitial quartz. Opaque minerals make-up ~10% of the groundmass and minor hornblende and biotite can be present. Secondary mineralisation includes metamorphic chlorite, muscovite and biotite. Some keratophyres also show rare orthoclase altered to chlorite and sericite alteration is common at the edges and within plagioclase phenocrysts.

4.3. Louisenhoj Formation

The basalts and andesites are largely porphyritic with vesicles in the andesites and amygdales in the basalts. Phenocrysts of stubby plagioclase, 3–5 mm, are abundant and contribute up to 50% of the samples. The plagioclase is predominately albitised. Clinopyroxene (10%) phenocrysts are also common in the samples of this study. The andesites also contain interstitial quartz and biotite within the groundmass and their amygdales are filled with chlorite, quartz and prehnite.

4.4. Tutu Formation

The basalts are porphyritic with abundant (up to 50%) phenocrysts of 3–4 mm long plagioclase. Clinopyroxenes are less common, but occur as larger phenocrysts up to 5 mm and are locally replaced by amphibole. The groundmass has a weak foliation because of the alignment of plagioclase and clinopyroxene together with minor amphibole (hornblende), chlorite and randomly distributed opaque minerals.

5. Geochemistry

5.1. Methodology

Thirty-seven samples from all of the pre-Eocene volcanic formations on St. John have been analysed for major and trace elements at Cardiff

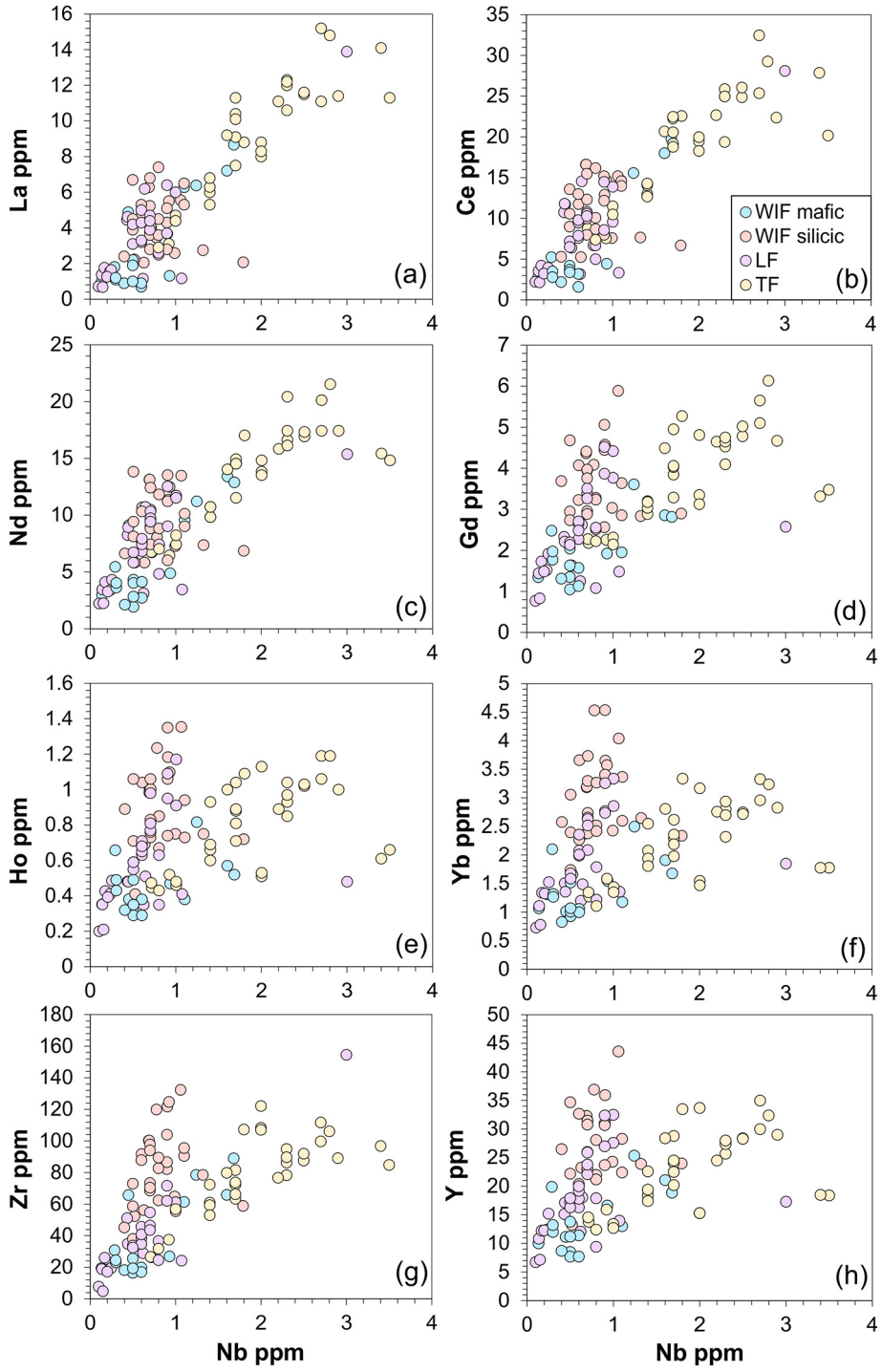

Fig. 2. Trace element bivariate plots for the WIF, LF and TF on St. John. Data are from this study and Jolly and Lidiak (2006).

University and a sub-set of twelve samples has been analysed for Nd–Hf radiogenic isotopes at Durham University (**Fig. A1 and Tables A1 and A2, Appendix**).

Following removal of weathered surfaces and obvious vein material the samples were crushed in a jaw crusher and powdered using an agate Tema ball mill. Approximately 2 g of powdered sample was heated in a porcelain crucible to 900 °C for two hours to determine the loss on ignition (LOI). For the chemical analysis, 0.1 g ±0.0005 of sample was mixed and fused with 0.4 g ± 0.0005 Li-metaborate flux. This was dissolved in a ~ 5% HNO_3 solution with a 1 ppm Rh spike and made up to 100 ml using 18 Ω distilled water. Major element concentrations were determined by using a JY Horiba Ultima 2 inductively coupled plasma optical emission spectrometer. 1 ml of the solution was further diluted with 1 ml of In and Tl spike and 8 ml of 2% HNO_3 and analysed using a Thermo X7 series inductively coupled plasma mass spectrometer to obtain trace element contents. The full major and trace element analytical procedure is described in McDonald and Viljoen (2006).

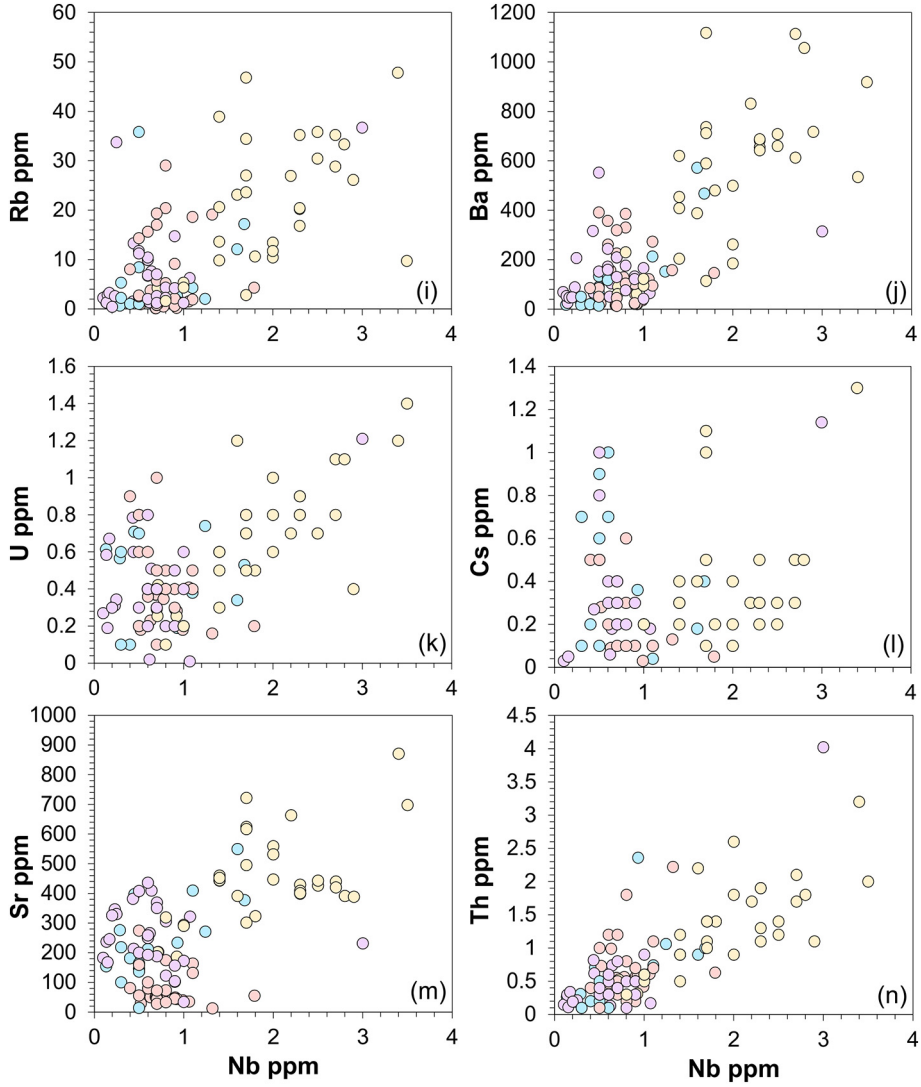

Fig. 2 (*continued*).

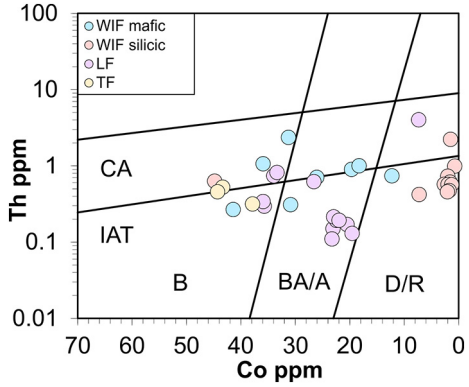

Fig. 3. Th–Co classification diagram from Hastie et al. (2007) showing the data determined in this paper. B, basalt; BA/A, basaltic andesite and andesite; D/R, dacite and rhyolite; IAT, island arc tholeiite; CA, calc-alkaline.

Nd-Hf radiogenic isotopes were determined at the Arthur Holmes Laboratory of the Durham Geochemistry Centre, Durham University. The samples were dissolved using standard HF-HNO_3 digestion followed by elemental pre-concentration based on the method of Dowall et al. (2007). Sample solutions were run through 1 ml pipette tips containing dilute Sr-spec resin to remove the Sr-bearing fractions. The high field strength element (HFSE)- and Rare Earth Element (REE)-bearing fraction was run through 10 ml polypropylene columns containing Bio-Rad AG50W-X8 200–400 mesh cation-exchange resin. Neodymium was collected as part of a general REE fraction. The HFSE-bearing fraction was then run through a 10 ml polypropylene column containing Bio-Rad AG1-X8 anion-exchange resin to separate Hf from Ti. All samples were taken up in 400–500 μl of 3% HNO_3. Radiogenic isotopes were analysed on a Thermo Neptune multi-collector inductively coupled plasma mass spectrometer. Neodymium was run with J&M and Sm-doped J&M standards giving a mean $^{143}Nd/^{144}Nd$ of 0.511104 ± 0.000011 (2σ, $n = 13$, uncertainty = 22.4 ppm). Results were normalised to a preferred value of 0.511110. Hf was run with standard JMC475 giving a mean $^{176}Hf/^{177}Hf$ of 0.282146 ± 0.000009 (2σ, $n = 9$, uncertainty = 31.3 ppm). Results were normalised to a preferred value of 0.282160. For the age correction of the samples we use the decay constants (λ): Lu-Hf = 1.876×10^{-11} and Sm-Nd = 6.54×10^{-12}. For chondritic values we use $^{143}Nd/^{144}Nd = 0.512638$, $^{147}Sm/^{144}Nd = 0.19670$, $^{176}Hf/^{177}Hf = 0.282772$ and $^{176}Lu/^{177}Hf = 0.03320$.

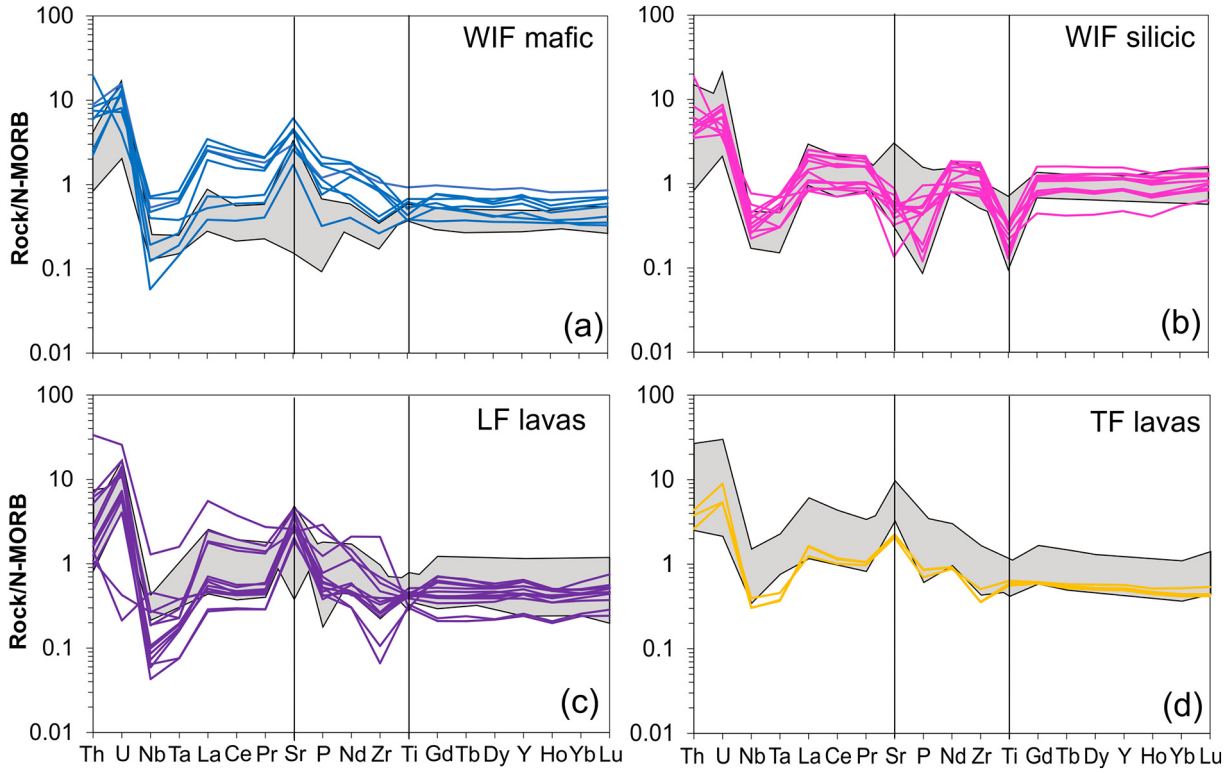

Fig. 4. N-MORB normalised multielement diagrams for all of the formations on St. John. Data from this paper and the grey fields represent data ranges from Jolly and Lidiak (2006). Normalising data are from Sun and McDonough (1989).

5.2. Element mobility and classification

Previous studies (e.g., Escuder Viruete and Castillo Carrión, 2016; Lidiak and Anderson, 2015; Neill et al., 2011; Torró et al., 2017) have shown that igneous rocks in the Caribbean region have suffered intense hydrothermal alteration and tropical weathering. As such, the large ion lithophile elements (LILE: K, Cs, Ba, Na) are frequently mobilised and cannot be used for petrogenetic interpretations. We can test the mobility of the LILE in rocks of the Virgin Islands by plotting bivariate diagrams with an element of interest on the ordinate and Nb on the abscissa. Niobium is plotted because it is one of the most immobile trace elements (e.g., Cann, 1970; Hill et al., 2000; Kurtz et al., 2000). If an element is plotted against Nb, the data should form a linear trend if the samples are co-genetic and the elements are moderately to highly incompatible and immobile.

Light rare earth element (LREE) bivariate diagrams show a broad and dominant positive liquid line of descent that demonstrates that the elements are incompatible, immobile and that the data could be consistent with a co-genetic petrogenesis for the entire St. John sample suite (Fig. 2a-c). However, the middle and heavy REE diagrams show the samples progressively forming three broad trends, as indicated on Fig. 2d-f. The M- and HREE should be immobile, therefore, the three trends suggest that the samples, as a whole suite, are not co-genetic. The silicic WIF and samples of the LF form a high M-HREE trend at a given Nb content and the TF forms a dominant middle trend. The Zr–Nb diagram shows two broad trends with the silicic WIF and TF samples forming low and high Zr liquid lines of descent at a given Nb content respectively (Fig. 2g). In contrast, the LILE data show relatively large amounts of scatter on the Rb, Ba, U and Cs–Nb bivariate plots in Fig. 2i-l that is consistent with the elements being mobilised during sub-solidus alteration. The trends appear more consistent on the Sr and Th–Nb diagrams and the Sr data shows very low Sr contents for the WIF silicic rocks.

In conclusion, the LILEs have been mobilised in the samples of this study, but Th, REE and HFSE are immobile and show relatively coherent liquid lines of decent (similar to other Caribbean igneous rocks, e.g., Marchesi et al., 2016). There are three broad magmatic trends seen in the bivariate diagrams and possibly several more distinct trends within the individual formations. However, two of the three broad trends are mostly represented by rocks of the TF and silicic WIF respectively. As such, the igneous rocks of St. John are not co-genetic, but are composed of multiple magmatic suites

Igneous rocks are routinely classified using the total alkali silica diagram, but because of the mobility of the LILEs in the St. John rocks we have opted to classify the samples using the immobile element Th–Co diagram of Hastie et al. (2007). The WIF mafic lavas mostly plot as tholeiitic and calcalkaline basalts and basaltic andesites while the WIF silicic rocks plot in the dacite/rhyolite field (Fig. 3). Similarly, the lavas of the LF predominantly classify as tholeiitic basalts to andesites and the rocks of TF are tholeiitic basalts (Fig. 3).

5.3. Multielement diagrams

Normal mid-ocean ridge basalt (N-MORB) normalised multielement plots in Fig. 4 show that all the rocks from St. John have large negative Nb–Ta anomalies. The WIF mafic rocks have predominantly MORB-like HREE contents, positive Sr anomalies and enriched Th and U (Fig. 4a). The silicic WIF also has MORB-like HREE, but the rocks have negative Sr, P and Ti anomalies (Fig. 4b). The LF rocks have relatively uniform HREE concentrations, but positive Sr anomalies and a wide range of incompatible element contents (Fig. 4c). The rocks of the TF have flat, MORB-like HFSE and HREE contents and a small positive Sr anomaly (Fig. 4d).

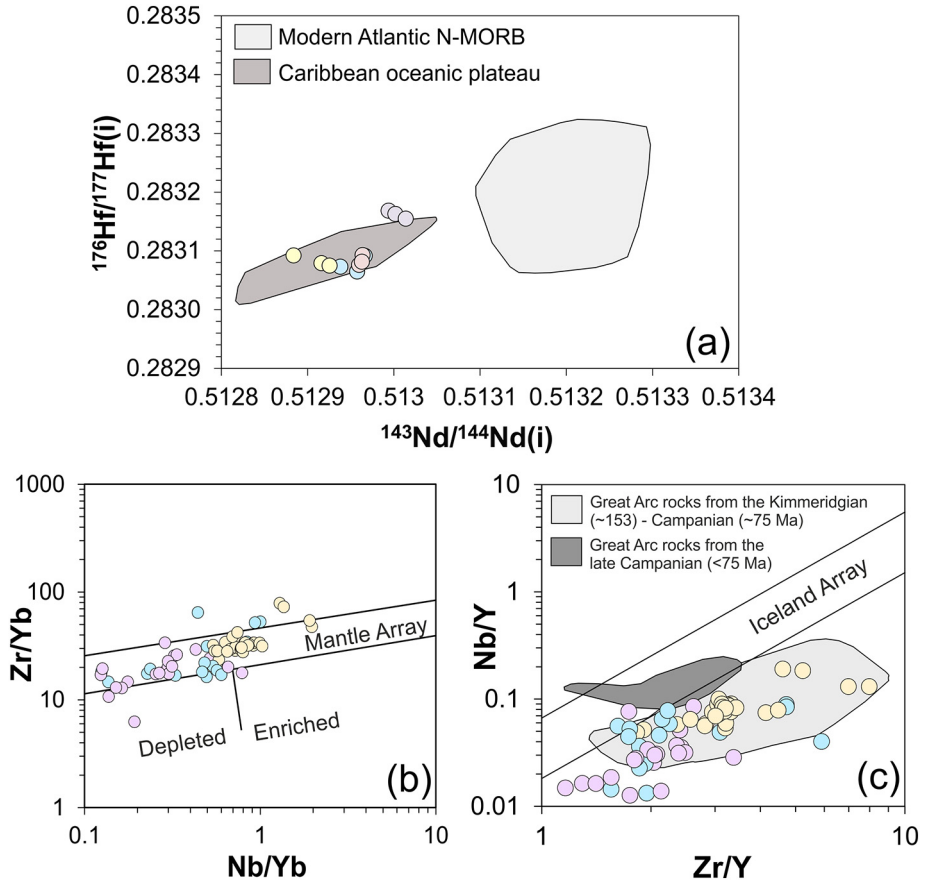

Fig. 5. (a) ^{176}Hf-$^{177}Hf(i)$ – $^{143}Nd/^{144}Nd(i)$ diagram with the modern Atlantic N-MORB field from Nowell et al. (1998) and the Caribbean plateau field from Hastie et al. (2016). (b) Zr/Yb-Nb/Yb diagram from Pearce and Peate (1995) showing the MORB-like character of the basic to intermediate rocks from St. John. (c) Nb/Y-Zr/Y diagram from Fitton et al. (1997) that implies no mantle plume component in the basic to intermediate rocks of St. John. Data in b and c are from this study and that of Jolly and Lidiak (2006).

5.4. Nd–Hf radiogenic isotopes

WIF mafic and silicic samples are age corrected to 100 Ma and samples from the LF and TF are corrected to 85 Ma. On an ^{176}Hf-$^{177}Hf(i)$ – $^{143}Nd/^{144}Nd(i)$ diagram (Fig. 5a) the three formations have distinctive radiogenic isotope compositions with LF rocks having the most depleted (radiogenic) values and the TF samples having the least depleted (non-radiogenic) composition. The three formations are geochemically distinct and are therefore derived from compositionally different mantle source regions.

6. Discussion

6.1. Nature of the mantle wedge

The main aim of this contribution is to determine the nature of the mantle component in the Cretaceous magmatic rocks of the Virgin Islands. In island arc magma petrogenesis the HFSE can be mobilised in slab-derived partial melts but are not mobilised easily by aqueous fluids from the dehydration of the slab (Keppler, 1996; Kessel et al., 2005; Pearce and Peate, 1995). Therefore, if the slab component in the St. John rocks is represented by a slab-fluid, the HFSE can be used to determine the compositional nature of the mantle wedge. We can test this for the Virgin Islands magmatic rocks in this study by plotting a Zr/Yb-Nb/Yb diagram from Pearce and Peate (1995) (Fig. 5b). Basic to intermediate samples from St. John lie within a defined mantle array. If Zr had been mobilised in a slab partial melt and added to the mantle wedge, the Zr/Y ratios of the St. John samples would plot above the mantle array. Fig. 5b shows that ratios of the HFSEs have not been mobilised in a slab-derived component (i.e., they are conservative) and so can be used to study the relative enrichment of the mantle source that underwent partial melting to form the St. John magmas.

Mantle plume-derived magmas are usually generated from less incompatible element depleted source regions than N-MORB and so have higher Nb concentrations. Therefore, on a Nb/Y-Zr/Y diagram, mantle plume-derived rocks have higher Nb/Y ratios at a given Zr/Y than N-MORB. This diagram was initially developed to investigate Icelandic lavas (Fitton et al., 1997) where enriched mantle plume rocks and N-MORB fall above and below a lower reference line respectively, but it works well for other mantle plume-derived rocks (e.g., Hastie et al., 2008). Data from basic and intermediate rocks from St. John and rocks from the U.S. Virgin Islands from Jolly and Lidiak (2006) are plotted in Fig. 5c. The samples lie below the lower reference line suggesting that the mantle component involved in the petrogenesis of the Cretaceous Virgin Island arc rocks had an N-MORB composition.

On the $^{176}Hf/^{177}Hf(i)$ – $^{143}Nd/^{144}Nd(i)$ diagram the St. John samples have more enriched (unradiogenic) compositions relative to modern N-MORB and they plot in the Caribbean oceanic plateau field (Fig. 5a). Nevertheless, unlike the HFSE, Nd is moderately non-conservative and will be mobilised in a slab-derived aqueous fluid (e.g., Keppler, 1996; Kessel et al., 2005; Pearce and Peate, 1995). Therefore, the St. John $^{143}Nd/^{144}Nd(i)$ values represent mixing between the mantle wedge source region and a slab-related component. The original St. John mantle compositions, prior to contamination with the slab-derived fluid, would have had higher (more radiogenic) $^{143}Nd/^{144}Nd(i)$ values. Therefore, it is likely, based purely on Nd–Hf radiogenic data, that the composition of the mantle wedge involved in the petrogenesis of the St. John

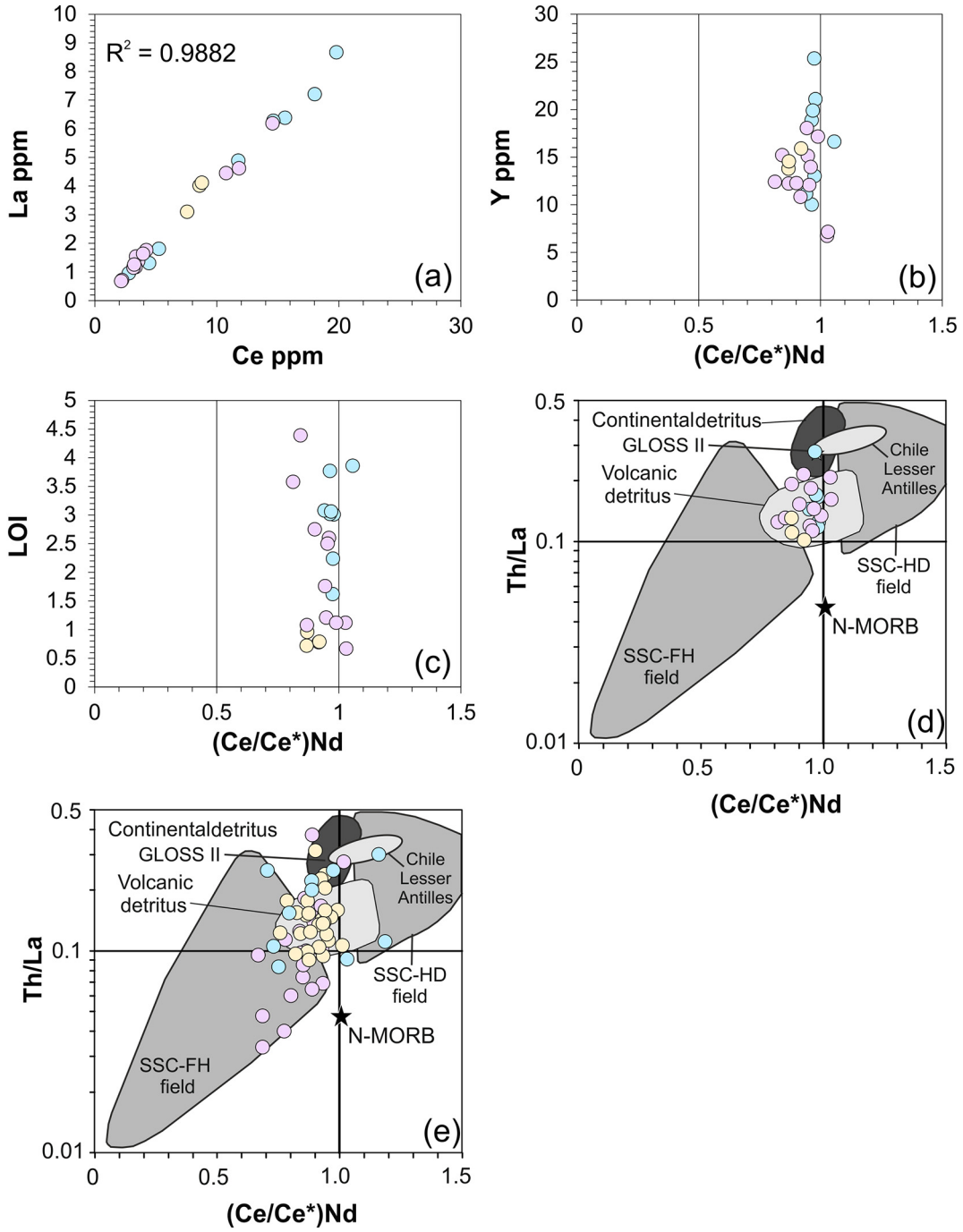

Fig. 6. (a-c) La–Ce, Y-$(Ce/Ce^*)_{Nd}$ and Loss on Ignition (LOI)-$(Ce/Ce^*)_{Nd}$ bivariate diagrams displaying data from this study. (d and e) Th/La-$(Ce/Ce^*)_{Nd}$ classification diagram from Hastie et al. (2013) showing data from this paper (d) and data from Jolly and Lidiak (2006) (e). GLOSS II, Global Subducting Sediment (Plank, 2014); SSC, Slow Sedimentation rate Clay; HD, Hydrogenous; FH, Fish debris and Hydrothermal.

magmas had a N-MORB composition; thus, supporting the Nb/Y-Zr/Y data.

6.2. Composition of the slab component

Many elements that are used to investigate the nature of slab components in island arc-derived lavas cannot be used in this study because they are mobilised during sub-solidus alteration processes (e.g., K and Ba: Elliott, 2003). However, Hastie et al. (2009, 2010, 2013) developed the Th/La-$(Ce/Ce^*)_{Nd}$ diagram that uses immobile trace elements to determine the geochemical components of the slab-derived flux in the petrogenesis of island arc magmatic rocks. Such fluxes could be composed of a variety of geochemical end members that include fluids from the basaltic crust, continental and volcanic detritus, and slow sedimentation-rate-clays (SSC). Such SSCs include hydrogenous Fe–Mn oxides, fish debris-rich clay and hydrothermal sediments.

The WIF silicic rocks on St. John have crystallised accessory allanite and apatite (Rankin, 2002). These Th and LREE-rich phases could potentially have an impact on the Th/La-$(Ce/Ce^*)_{Nd}$ diagram; thus, only basic to intermediate samples from the WIF, LF and TF are plotted. Furthermore, sub-solidus alteration processes can preferentially mobilise REE^{3+} and Y, relative to Ce^{4+}. Therefore, the hydrothermal fluids

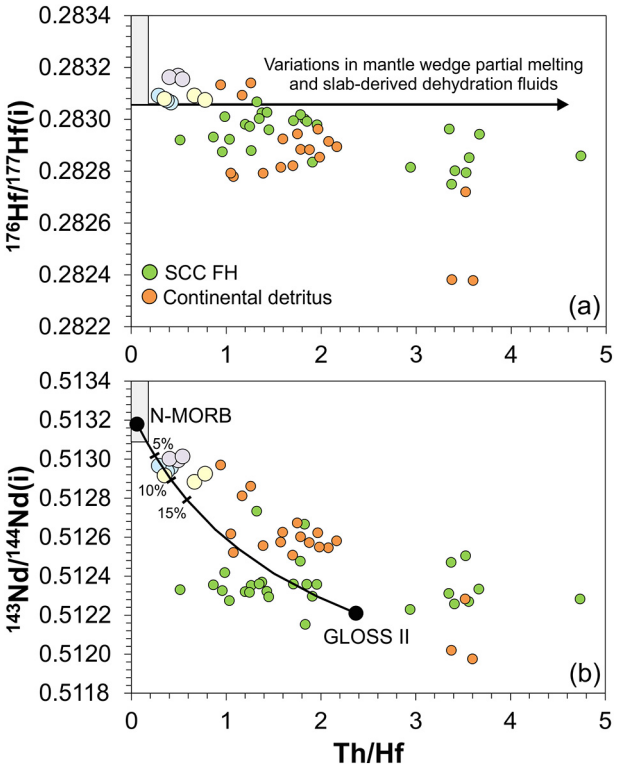

Fig. 7. ^{176}Hf-^{177}Hf(i) – Th/Hf and ^{143}Nd/^{144}Nd(i) – Th/Hf diagrams with modern Atlantic N-MORB field from Nowell et al. (1998) and the sedimentary data derived from Plank (2014) and Vervoort et al. (2011).

responsible for sub-solidus alteration can impart negative and positive Ce anomalies depending on whether the fluid has been removed or added to the rock (Cotten et al., 1995; Patino et al., 2003). Basic-intermediate rocks analysed in this study are plotted on a La–Ce bivariate diagram that shows a linear trend with $R^2 = 0.99$ (Fig. 6a). If any Ce anomalies in the St. John dataset are formed by variable metasomatism of REE^{3+} fluids the La–Ce ratio would be expected be variable and not show a linear correlation coefficient close to unity. Hydrothermal alteration would also disturb Y concentrations and may lead to high loss of ignition values (LOI) if the rocks have not been extensively silicified. The St. John samples do not show systematic correlations between Y or LOI versus $(Ce/Ce^*)_{Nd}$ (Fig. 6b and c); thus, suggesting that Ce anomalies in the St. John samples are unrelated to secondary alteration processes.

The St. John samples analysed in this study are plotted on the Th/La-$(Ce/Ce^*)_{Nd}$ diagram and are interpreted to be generated predominantly by mixing between a mantle-like component and continental detritus (Fig. 6d). The average Th/La values for the basic to intermediate samples of the WIF and LF are 0.16 (not including sample SJ52 that has anomalously high values) and 0.11 for rocks of the TF. This suggests that WIF and LF magmas contain a higher proportion of, or a more enriched, continental detritus component than the TF magmas. Furthermore, some of the samples are slightly displaced to lower $(Ce/Ce^*)_{Nd}$ values, which implies a small contribution from a SSC component rich in fish debris and/or hydrothermal sediments. The average $(Ce/Ce^*)_{Nd}$ values for the basic to intermediate samples from the WIF and LF range from 0.93–0.97 (again, not including sample SJ52), but the TF rocks are relatively low with 0.89. Therefore, this implies that the TF magmas contain a higher proportion of, or a more $(Ce/Ce^*)_{Nd}$ depleted, SSC component than the WIF and LF magmas.

These findings are generally supported by Virgin Island data in Jolly and Lidiak (2006) where WIF, LF and TF mafic rocks form a broad mixing array between a mantle component and continental detritus (Fig. 6e). However, the Jolly and Lidiak (2006) TF data have a higher average Th/La ratio of 0.15 and the LF have a low ratio of 0.12. All the samples are displaced to relatively low $(Ce/Ce^*)_{Nd}$ values with WIF, LF and TF having 0.85–0.91. In particular, some of the LF rocks have very low $(Ce/Ce^*)_{Nd}$ values down to 0.67. Consequently, data in this study and in Jolly and Lidiak (2006) suggest that all the formations show evidence of variable contributions from both continental detritus and fish debris and/or hydrothermal sediments.

The St. John lavas do not have adakite compositions, which would be expected if the slab component was a partial melt derived from the magmatic portion of the subducting plate. A partial melt from any sedimentary veneer would mobilise the HFSEs, which is not seen in Fig. 5b. In addition, a ^{176}Hf/^{177}Hf(i) – Th/Hf diagram is shown in Fig. 7a, and if the slab component was a sedimentary melt, the St. John samples would be expected to be displaced to lower ^{176}Hf/^{177}Hf(i) and higher Th/Hf ratios due to the mobility of Th and Hf in a slab-derived sedimentary melt. In contrast, Nd does not require a slab melt because it will be mobilised during slab dehydration (Pearce and Peate, 1995) and the St. John ^{143}Nd/^{144}Nd(i) values will represent mixing between the mantle wedge and the slab fluid. Fig. 5a shows that the TF is relatively more enriched in ^{143}Nd/^{144}Nd(i) relative to WIF, and LF and WIF is slightly more enriched than LF. Thus, if the Jolly and Lidiak (2006) database is combined with our new analyses, Th/La and $(Ce/Ce^*)_{Nd}$ suggest that there is no simple case where one formation dominantly shows evidence for a stronger association with either a continental or SSC slab-derived component. However, ^{143}Nd/^{144}Nd(i) values demonstrate that the TF has been contaminated with either a larger proportion of, or a more enriched sedimentary slab-derived component relative to WIF and LF samples.

As with previous studies, it is difficult to model this mixing because we do not know the nature of the sediments that were subducting beneath the Great Arc ~127–85 Ma. However, if we assume a mixture between N-MORB (Sun and McDonough, 1989) and the Global Subducting Sediment (GLOSS II) end member of Plank (2014) we can model the generation of the St. John rocks using a ^{143}Nd/^{144}Nd(i) – Th/Hf diagram (Fig. 7b). For the radiogenic isotope data, the mixing curve is calculated by:

$$C_M = \frac{C_A{}^{143/144}(C_A X) + C_B{}^{143/144}(C_B(1-X))}{C_A X + (C_B(1-X))} \quad (1)$$

where C_M is the ^{143}Nd/^{144}Nd(i) value of the mixture, $C_A^{143/144}$ and $C_B^{143/144}$ are the ^{143}Nd/^{144}Nd(i) ratios in components A and B respectively, C_A and C_B represent the corresponding Nd concentrations of components A and B respectively, and X is the mass fraction of component A in the mixture (DePaolo, 1981). Also, the Th and Hf mixing concentrations are calculated by:

$$C_M = C_A X + C_B(1-X) \quad (2)$$

where C_M is the concentration of Th or Hf in the mixture, C_A and C_B are the abundances of Th or Hf in components A and B respectively, and X is the proportion of component A. The mixing curve shows that the compositions of the St. John island arc rocks can be replicated with a mixture of 95–85% N-MORB and 5–15% GLOSS II, with samples from the TF requiring a larger percentage of GLOSS II.

6.3. Petrogenesis of the WIF silicic rocks

The silicic rocks of the WIF could have been formed by either large degrees of fractional crystallisation of mafic parental magmas or the partial melting of mafic source rocks in the lower arc basement (Jolly et al., 2008; Jolly and Lidiak, 2006). The similarity of the ^{76}Hf/^{177}Hf (i) and ^{143}Nd/^{144}Nd(i) ratios strongly suggests that the WIF mafic rocks represent either the parental magmas or the source rocks for the WIF silicic rocks (Fig. 6a).

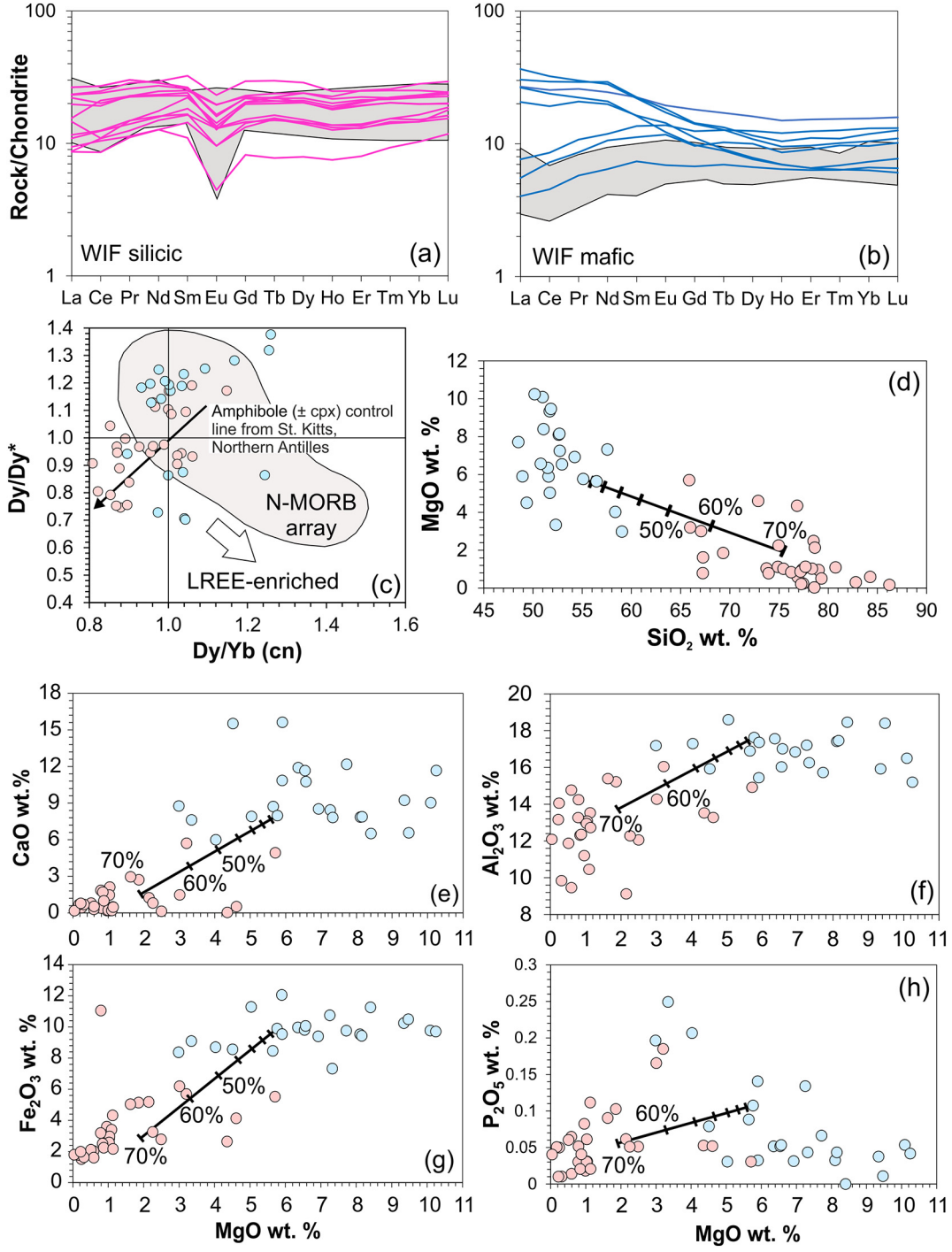

Fig. 8. (a and b) Chondrite-normalised REE diagrams showing raw data from this study and grey fields representing analyses from Jolly and Lidiak (2006). (c) Dy/Dy*-Dy/Yb diagram from Davidson et al. (2013) and (d-h) major element bivariate diagrams showing fractional crystallisation trends of a plagioclase (58%), clinopyroxene (10%), magnetite (12%), orthopyroxene (10%), amphibole (9.7%) and apatite (0.3%) mineral assemblage from a parental magma representing WIF sample SJ53. Tick marks on trends represent 10% increments. Virgin Island data in c-h are from this paper and Jolly and Lidiak (2006). Normalising values from McDonough and Sun (1995).

Chondrite-normalised REE diagrams in Fig. 8a and b show that the rocks of the WIF have slight concave-up patterns that is frequently interpreted as due to amphibole-controlled fractionation by either crystallisation from a magma or as a residual phase in a metabasic source region. To quantify such patterns Davidson et al. (2013) developed the Dy/Dy* [chondrite normalised (cn) $Dy/(La^{4/13} \times Yb^{9/13})$] versus Dy/Yb_{cn} diagram. A MORB field on this diagram extends from low $Dy/Yb_{cn} < 1$ and $Dy/Dy^* > 1$ to low $Dy/Dy^* < 1$ and $Dy/Yb_{cn} > 1$ (Fig. 8c). Primitive arc magmas plot in the MORB field and subsequent amphibole (± cpx) fractional crystallisation should lead to the generation of more evolved arc magmas with *both* Dy/Dy^* and $Dy/Yb_{cn} < 1.0$. Fig. 8c shows the WIF mafic rocks predominantly plotting in the MORB array. Some of the mafic samples plot with Dy/Dy^* ratios <1 and these represent the small number of samples in Fig. 8b that are relatively enriched in LREE compared to HREE. However, the majority of the mafic WIF rocks are relatively depleted in LREE and have Dy/Dy^* ratios >1. The WIF silicic rocks plot on a moderately linear trend from the LREE-depleted mafic rocks to compositions with Dy/Dy^* and

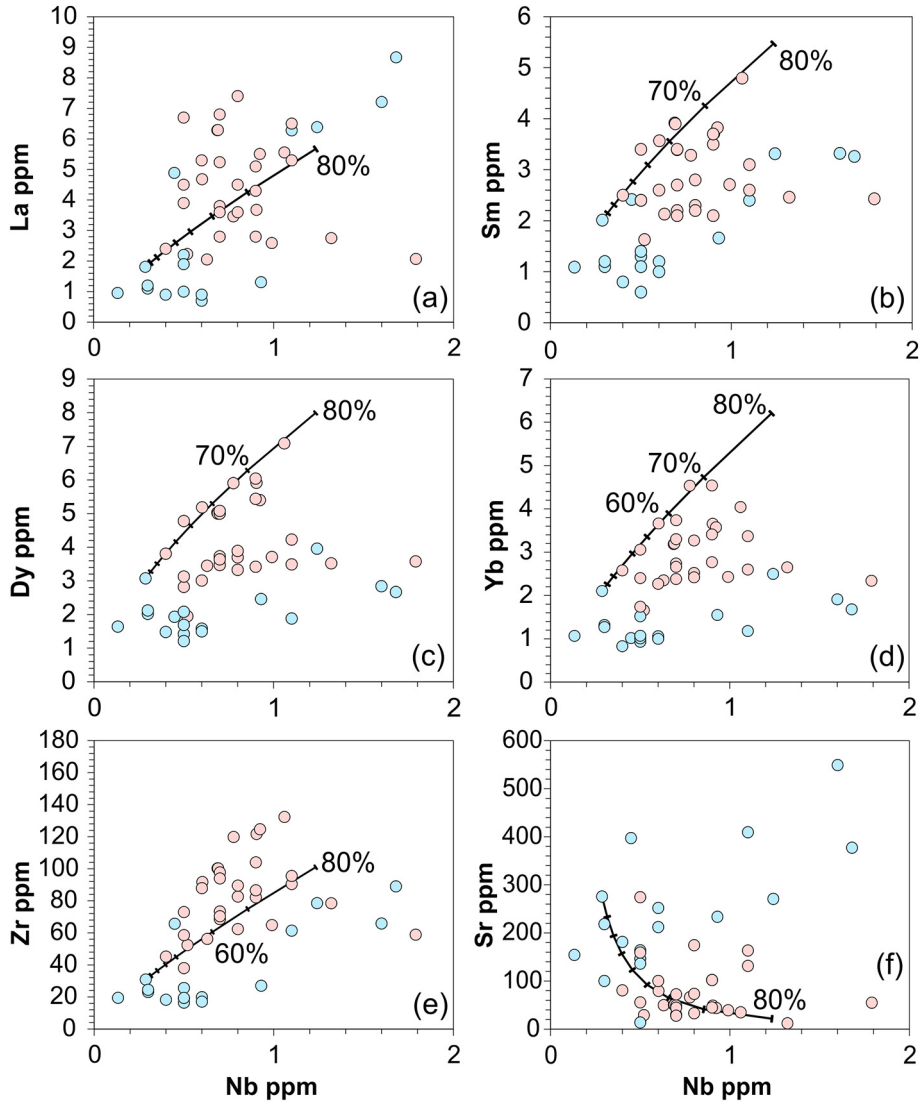

Fig. 9. (a-f) Selected trace element variation diagrams showing fractional crystallisation trends of a plagioclase (58%), clinopyroxene (10%), magnetite (12%), orthopyroxene (10%), amphibole (9.7%) and apatite (0.3%) mineral assemblage from a parental magma representing WIF sample SJ53. D values are taken from Fujimaki et al. (1984), McKenzie and O'Nions (1991), Bacon and Druitt (1988) and Bédard (2006). Tick marks on trends represent 10% increments.

Dy/Yb(cn) <1. This suggests that amphibole controlled fractional crystallisation of the WIF mafic rocks can form the silicic samples. It also shows that no garnet is involved as garnet fractionation would increase Dy/Yb(cn).

Woodhead (1988) modelled the formation of intra-oceanic island arc lavas by fractional crystallisation processes using a mineral assemblage of plagioclase, clinopyroxene, magnetite and olivine in the proportions 60:25:10:5 respectively. Evidence of plagioclase and magnetite crystallisation in the silicic WIF is apparent with low Sr (Fig. 2m) and Fe contents (not shown). The intermediate Virgin Island rocks that could represent the parental magmas for the keratophyres would be too silicic for olivine saturation and would instead crystallise orthopyroxene. Finally, the negative P anomalies in the keratophyres (Fig. 4) suggests that apatite was also crystallising. Therefore, we have modified the crystallisation mode of Woodhead (1988) to include plagioclase, clinopyroxene, magnetite, orthopyroxene, amphibole and apatite in proportions of 58:10:12:10:9.7:0.3. We have calculated the removal of this bulk mineral assemblage from a theoretical WIF intermediate magma by mass balance using the following equation:

$$C_l = \frac{C_0 - (C_{min}X)}{1 - X} \quad (3)$$

where C_l is the concentration of the magma after a given proportion of crystallisation, C_0 is the original magma composition that is taken as that of the relatively evolved mafic sample SJ53, C_{min} is the composition of the bulk mineral assemblage being removed from the magma and X is the mass fraction of the mineral assemblage being removed. Calculated major element liquid lines of decent in Fig. 8d-h show that it is possible to generate silicic WIF igneous rocks from an intermediate WIF parent through the removal of ~50–70% of the crystallising assemblage

We have tested the major element crystallisation results by modelling the evolution of trace element concentrations during fractional crystallisation of the same parental intermediate WIF magma using the equation:

$$C_l = C_0 F^{(D-1)} \quad (4)$$

C_l and, C_0 are as in Eq. (3), D is the bulk partition coefficient of the fractionating assemblage using partition coefficients from Fujimaki

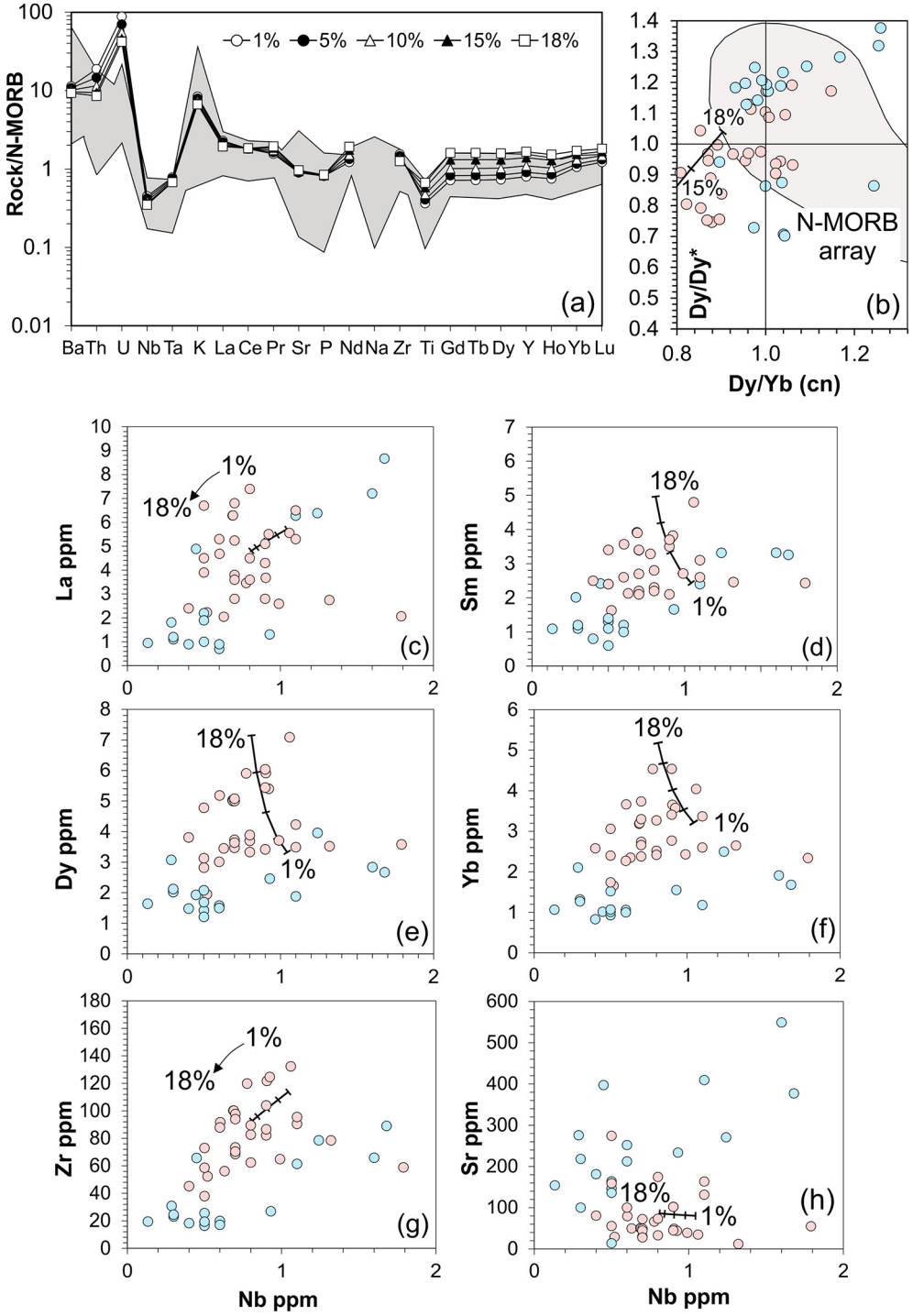

Fig. 10. (a) N-MORB normalised multielement plot showing the results of partial melting of a garnet-free metabasic source region using SJ53 as the starting composition. The starting mode includes plagioclase (0.4973), amphibole (0.3261), quartz (0.0854), clinopyroxene (0.002) orthopyroxene (0.0136), magnetite (0.0531), ilmenite (0.02) and apatite (0.0025) and the melt modes are plagioclase (0.2641), amphibole (1.747), quartz (0.4576), clinopyroxene (−1.0755) orthopyroxene (−0.2983), magnetite (−0.0994), ilmenite (0.0021) and apatite (0.0025). Both the mineral and melt modes are taken from Beard and Lofgren (1991). The non-modal batch equation is used from Shaw (1970) and D values are derived from Bédard (2006). (b) Dy/Dy*-Dy/Yb diagram from Davidson et al. (2013) showing the metabasic partial melting trend intersects the silicic WIF data with ~10–18% partial melting. (c-h) Selected trace element variation diagrams showing partial melt trends for the arc composition from Beard and Lofgren (1991). Partial melt fractions range from 1 to 18% and the internal increments represent 5, 10 and 15%. Virgin Island data are derived from this paper and Jolly and Lidiak (2006). Normalising values from Sun and McDonough (1989).

et al. (1984), McKenzie and O'Nions (1991), Bacon and Druitt (1988) and Bédard (2006) and F is the proportion of melt remaining. Fractional crystallisation trends in Fig. 9a-f show that the trace element abundances of the keratophyres can be explained by 50–70% crystallisation of a WIF intermediate parental magma. Also, the models show that Dy/Dy* and Dy/Yb(cn) <1 can be replicated and the whole compositional range of the silicic rocks can be formed by the evolution of the compositionally heterogeneous WIF mafic rocks. Finally, the low

proportion of crystallising apatite in our models does not have any substantial effect on the Dy/Yb and Dy/Dy* ratios that we use to justify amphibole removal.

Nevertheless, Jolly and Lidiak (2006) suggest that the lack of intermediate magmatism and the overwhelming volume of silicic (80%) compared to mafic material (20%) (Fig. 1d) implies that the keratophyres are most likely generated by crustal fusion. We have tested this crustal fusion scenario by modelling the partial melting of a theoretical garnet-free metabasic source region. The low Dy/Dy* and Dy/Yb(cn) ratios suggest that amphibole is required in the residue and so an anhydrous pyroxenite source region is unsuitable. The non-modal partial melt equation from Shaw (1970) is used for the calculation:

$$C_l = \frac{C_0}{D + F(1-P)} \quad (5)$$

where C_l is the concentration of the resultant melt, C_0 is the concentration of the source region before partial melting (taken as SJ53 again), F is the mass fraction of melt generated, D is the bulk partition coefficient prior to partial melting and P is the average of the partition coefficients weighted by the proportion contributed by each phase to the melt.

The starting mineral and melt modes are from Beard and Lofgren (1991) because they supply data for the partial melting of low-pressure, garnet-free amphibolites from an arc setting. The mineral mode includes plagioclase, amphibole, magnetite, quartz, clinopyroxene, orthopyroxene and ilmenite. We slightly modify this modal proportion by adding apatite that is required to generate relatively low P concentrations in the keratophyres (Fig. 4). The starting mode comprises plagioclase (0.4973), amphibole (0.3261), quartz (0.0854), clinopyroxene (0.002) orthopyroxene (0.0136), magnetite (0.0531), ilmenite (0.02) and apatite (0.0025) and the melt mode comprises plagioclase (0.2641), amphibole (1.747), quartz (0.4576), clinopyroxene (−1.0755) orthopyroxene (−0.2983), magnetite (−0.0994), ilmenite (0.0021) and apatite (0.0025). The melt mode indicates that amphibole and quartz would be exhausted after ~18% partial melting; thus we restrict the range of modelled melts in **Fig. 10** to 1–18%. Our calculations show that the WIF silicic multielement patterns, Dy/Dy* and Dy/Yb(cn) ratios <1 and trace element abundances on bivariate diagrams can be replicated by ~1–18% partial melting of a WIF mafic source region (Fig. 10a-h).

Although we have shown that the composition of the WIF silicic rocks can be generated by partial melting of a relatively shallow metabasic source region with compositions similar to the WIF mafic rocks, geochemical modelling can also support a fractional crystallisation model for generating the keratophyres. Distinguishing between the two processes is extremely difficult; however, we favour the partial melt process due to the relatively large volumes of silicic material and lack of intermediate compositions.

6.4. Geochemical summary

The Barremian to Santonian (127–83.6 Ma) St. John rocks in this study represent pre- and post-COP island arc magmatism that has IAT and CA compositions. All the rocks, except for the silicic WIF samples, have immobile trace element and Nd–Hf radiogenic isotope ratios that show that the St. John samples are derived from the partial melting of an Atlantic MORB-like mantle source region that has been variably contaminated with slab-derived fluids composed of continental detritus and slow sediment clay components. In contrast to younger Campanian (83.6–72.1 Ma) igneous rocks in the Great Arc (e.g., Hastie et al., 2013), none of the rocks from St. John show evidence for a mantle plume-like geochemical signature.

6.5. Evolution of the Inter-American region in the cretaceous

It has been proposed that Caribbean lithosphere moved into the inter-American region in the Hauterivian-Albian (132.9–100.5 Ma) (Boschman et al., 2014; Marchesi et al., 2016; Pindell et al., 2011; Pindell and Kennan, 2009; Torró et al., 2016, 2017). If so, partial melting in the convergent margin with southwest-directed subduction would likely tap mantle plume-like material instead of depleted MORB mantle after ~90 Ma. Hastie et al. (2013) showed that such a mantle plume signature is not seen in island arc igneous rocks throughout the Caribbean until after the late Campanian (<75 Ma) (Fig. 5c). Similarly, Barremian to Santonian (127–83.6 Ma) island arc magmatic rocks on St. John show no geochemical evidence for the involvement of a mantle plume and, thus, a COP component before the Santonian. This is surprising because our younger samples post-date the 94–88 Ma COP and would be expected to show an oceanic plateau signature with southwest-directed subduction. This indicates that, before ~84 Ma, subduction in the inter-American region was most likely to the northeast and magmatism was generated by partial melting a mantle wedge composed of Atlantic-like N-MORB.

In keeping with our earlier conclusions (e.g., Hastie and Kerr, 2010), we still maintain that one of the major problems with an Early Cretaceous reversal is that the Farallon plate was subducting to the east and beneath the Americas since the Permian (e.g., Mann et al., 2007; Spikings et al., 2015). Relatively localised southwest-directed subduction of the proto-Caribbean oceanic crust in the Early Cretaceous would lead to a serious space problem. Regardless of what mechanism is invoked in the overlying American and Proto-Caribbean lithosphere to initiate subduction reversal, the underlying Farallon plate would have continued to subduct to the northeast. To allow the proto-Caribbean lithosphere to be consumed in a southwest-directed subduction zone the Farallon plate must be locally prevented from subducting to the northeast. The Turonian-Campanian (93.9–72.1 Ma) hypothesis satisfies these constraints because the collision of the COP with the Great Arc would jam the subduction zone and prevent the Farallon plate from locally subducting in the inter-American region. This allows both subduction reversal and subduction back-step to isolate the COP and the Great Arc and results in the development of the Caribbean plate. In contrast, models that invoke an early Cretaceous reversal have to explain how the Farallon plate is prevented from locally subducting to the northeast. A further problem with early Cretaceous reversal involves the potential southwest-directed subducting plate at depth in the mantle. If oceanic lithosphere was subducting to the southwest from ~130–100 Ma and the mantle plume that generated the Caribbean oceanic lithosphere is dominantly 88–90 Ma the southwest-directed slab at depth may prevent mantle plume material from being emplaced close to the active island arc. This may particularly be true if young Proto-Caribbean lithosphere subducted at a relatively shallow angle. Nevertheless, we note that the formation of southwest-directed subduction further to the west in an intra-oceanic island arc would help negate a space problem. Indeed, Boschman et al. (2019) advocate that a convergent margin with southwest-directed subduction could form at ~125 Ma to the west of existing northeast-directed subduction between the Americas. The two subduction zones subsequently collide at ~100 Ma to locally reverse northeast-directed subduction in the Proto-Caribbean region. However, forming a subduction zone is very difficult. It is easier for India to underthrust the Himalaya than it is to form a subduction zone to the south of Kerala. Slab pull will be pulling old and thick oceanic lithosphere below the Americas at 135–100 Ma in a northeast-direction. Why and how would very thick and very old oceanic lithosphere to the west of the Americas locally suddenly stop being pulled to the northeast, break and then reverse direction to subduct to the southwest?

We continue to argue that before the Turonian to Campanian (93.9–72.1 Ma) a northeast directed subduction zone existed along

the western seaboard of the Americas generating the Great Arc of the Caribbean (Hastie et al., 2013). In the late Cretaceous (~88–94 Ma) the main volume of the COP erupted onto the Farallon plate. The plateau was then transported to the northeast and collided with the Great Arc of the Caribbean. The collision choked the northeast-directed subduction zone and generated a subduction polarity reversal at ~80–75 Ma where southwest-directed subduction initiated on the eastward seaboard of the Great Arc. The movement of the COP between the American continents in the Turonian-Campanian (93.9–72.1 Ma) would have reduced or prevented the flow of oxygenated bottom water through the inter-American passage (Buchs et al., 2018; Kerr, 1998). This may have been the causal mechanism of, or at least contributed to, the formation of the Cenomanian-Turonian mass extinction event that is evidenced by a global oceanic anoxia event at this time (OAE-2) and also continued anoxic events up to the Santonian (OAE-3) (Buchs et al., 2018; Kerr, 2005).

7. Conclusions

Cretaceous igneous island arc rocks on St. John, U.S. Virgin Islands are Barremian (127 Ma) to Santonian (83.6 Ma) in age. The rocks are derived from partial melting an Atlantic MORB-like mantle source region that has been variably contaminated with slab fluids with dissolved continental detritus and slow-sediment clays. The most silicic rocks can be modelled with fractional crystallisation processes from more primitive parental magmas and also by partial melting of a low-pressure metamorphosed basaltic source region. However, the relatively large volumes of silicic material relative to mafic and intermediate compositions and lack of intermediate compositions favour a partial melt origin. The lack of mantle plume geochemical signature in the arc rocks strongly suggests that the translation of Caribbean lithosphere into the inter-American region occurred in the late Cretaceous (post-Santonian) due to a subduction polarity reversal caused by collision of the COP with the Great Arc.

Declaration of Competing Interest

The authors declare that they have no known competing financial interests or personal relationships that could have appeared to influence the work reported in this paper.

Acknowledgements

Alan Hastie acknowledges NERC PhD Studentship NER/S/A/2003/11215. The funding for the Nd and Hf radiogenic isotope work at Durham University came from a small grant from the Centre for Earth and Environmental Science Research at Kingston University, London. We thank Geoff Nowell for all his help for the analyses. Douglas W Rankin, Edward Lidiak and Wayne Jolly are also thanked for extremely valuable help and advice on fieldwork and sample collecting on St. John. Prof. Lidiak kindly supplied two of the Tutu samples for Nd–Hf analysis. Finally, we are grateful to Godfrey Fitton who commented on a draft of this manuscript and to L. Boschman and an anonymous reviewer for thorough and constructive feedback.

Appendix A. Supplementary data

Supplementary data to this article can be found online at https://doi.org/10.1016/j.lithos.2021.105998.

References

Bacon, C.R., Druitt, T.H., 1988. Compositional evolution of the zoned calcalkaline magma chamber of Mount Mazama, Crater Lake, Oregon. Contrib. Mineral. Petrol. 98, 224–256.

Beard, J.S., Lofgren, G.E., 1991. Dehydration melting and water-saturated melting of basaltic and andesitic greenstones and amphibolites at 1, 3, and 6·9 kb. J. Petrol. 32, 365–401.

Bédard, J.H., 2006. A catalytic delamination-driven model for coupled genesis of Archaean crust and sub-continental lithospheric mantle. Geochim. Cosmochim. Acta 70, 1188–1214.

Boschman, L.M., van Hinsbergen, D.J.J., Torsvik, T.H., Spakman, W., Pindell, J.L., 2014. Kinematic reconstruction of the Caribbean region since the Early Jurassic. Earth Sci. Rev. 138, 102–136.

Boschman, L.M., van der Wiel, E., Flores, K.E., Langereis, C.G., van Hinsbergen, D.J.J., 2019. The Caribbean and Farallon Plates connected: constraints from stratigraphy and paleomagnetism of the Nicoya Peninsula, Costa Rica. J. Geophys. Res. Solid Earth 124, 6243–6266.

Buchs, D.M., Kerr, A.C., Brims, J.C., Zapata-Villada, J.P., Correa-Restrepo, T., Rodríguez, G., 2018. Evidence for subaerial development of the Caribbean oceanic plateau in the Late Cretaceous and palaeo-environmental implications. Earth Planet. Sci. Lett. 499, 62–73.

Burke, K., 1988. Tectonic evolution of the Caribbean. Ann. Rev. Earth Planet. Sci. Lett. 16, 201–230.

Cann, J.R., 1970. Rb, Sr, Y, Zr and Nb in some ocean floor basaltic rocks. Earth Planet. Sci. Lett. 10, 7–11.

Cotten, J., Le Dez, A., Bau, M., Caroff, M., Maury, R.C., Dulski, P., Fourcade, S., Bohn, M., Brousse, R., 1995. Origin of anomalous rare-earth element and yttrium enrichments in subaerially exposed basalts: evidence from French Polynesia. Chem. Geol. 119, 115–138.

Davidson, J., Turner, S., Plank, T., 2013. Dy/Dy*: variations arising from mantle sources and petrogenetic processes. J. Petrol. 54, 525–537.

DePaolo, D.J., 1981. Trace element and isotopic effects of combined wallrock assimilation and fractional crystallization. Earth Planet. Sci. Lett. 53, 189–202.

Donnelly, T.W., Rogers, J.J.W., 1980. Igneous series in Island Arcs: the Northeastern Caribbean compared with Worldwide Island Arc assemblages. Bull. Volcanol. 43, 347–382.

Donnelly, T., Rogers, J., Pushkar, P., Armstrong, R., 1971. Chemical evolution of the igneous rocks of the eastern West Indies: an investigation of thorium, uranium, and potassium distributions and lead and strontium isotopic ratios. In: Donnelly, T. (Ed.), Caribbean Geophysical, Tectonic, and Petrologic Studies. Geological Society of America Memoir. Geological Society of America, Boulder, pp. 181–224.

Donnelly, T.W., Beets, D., Carr, M.J., Jackson, T., Klaver, G., Lewis, J., Maury, R., Schellenkens, H., Smith, A.L., Wadge, G., Westercamp, D., 1990. History and tectonic setting of Caribbean magmatism. In: Dengo, G., Case, J.E. (Eds.), The Geology of North America, The Caribbean Region. Geological Society of America Volume H, pp. 339–374.

Dowall, D.P., Nowell, G.M., Pearson, D.G., 2007. Chemical pre-concentration procedures for high-precision analysis of Hf-Nd-Sr isotopes in geological materials by plasma ionisation multi-collector mass spectrometry (PIMMS) techniques. In: Holland, J.G., Tanner, S.D. (Eds.), Plasma Source Mass Spectrometry: Applications and Emerging Technologies. The Royal Society of Chemistry, Cambridge, pp. 321–337.

Duncan, R.A., Hargraves, R.B., 1984. Plate tectonic evolution of the Caribbean region in the mantle reference frame. In: Bonini, W.E., Hargraves, R.B., Shagam, R. (Eds.), The Caribbean-South America Plate Boundary and Regional Tectonics. Geological Society of America Memoir vol. 162, pp. 81–93.

Edgar, N.T., Ewing, J.I., Hennion, J., 1971. Seismic Refraction and Reflection in the Caribbean Sea. 55. American Association of Petroleum Geologists, pp. 833–870.

Elliott, T., 2003. Tracers of the Slab. Inside the subduction factory. Geophys. Monogr. Series 138, 23–45.

Escuder Viruete, J., Castillo Carrión, M., 2016. Subduction of fore-arc crust beneath an intra-oceanic arc: the high-P Cuaba mafic gneisess and amphibolites of the Rio San Juan Complex. Lithos 262, 298–319.

Escuder Viruete, J., Díaz de Neira, A., Hernáiz Huerta, P.P., Monthel, J., García Senz, J., Joubert, M., Lopera, E., Ullrich, T., Friedman, R., Mortensen, J., Pérez-Estaun, A., 2006. Magmatic relationships and ages of Caribbean Island arc tholeiites, boninites and related felsic rocks, Dominican Republic. Lithos 90, 161–186.

Escuder Viruete, J., Joubert, M., Urien, P., Friedman, R., Weis, D., Ullrich, T., Pérez-Estaún, A., 2008. Caribbean island-arc rifting and back-arc basin development in the Late Cretaceous: geochemical, isotopic and geochronological evidence from Central Hispaniola. Lithos 104, 378–404.

Escuder Viruete, J., Pérez-Estaún, A., Weis, D., Friedman, R., 2010. Geochemical characteristics of the Río Verde Complex, Central Hispaniola: implications for the paleotectonic reconstruction of the lower Cretaceous Caribbean island-arc. Lithos 114, 168–185.

Fitton, J.G., Saunders, A.D., Norry, M.J., Hardarson, B.S., Taylor, R.N., 1997. Thermal and chemical structure of the Iceland plume. Earth Planet. Sci. Lett. 153, 197–208.

Frost, C.D., Schellekens, J.H., Smith, A.L., 1998. Nd, Sr, and Pb isotopic characterization of Cretaceous and Paleogene volcanic and plutonic island arc rocks from Puerto Rico. In: Lidiak, E.G., Larne, D.K. (Eds.), Tectonics and Geochemistry of the Northeast Caribbean. Geological Society of America, Special Papers vol. 322, pp. 123–132.

Fujimaki, H., Tatsumoto, M., Aoki, K.-i, 1984. Partition coefficients of Hf, Zr, and REE between phenocrysts and groundmasses. J. Geophys. Res. 89, 662–672.

Hastie, A.R., 2009. Is the Cretaceous primitive island arc (PIA) series in the circum-Caribbean region geochemically analogous to the modern island arc tholeiite (IAT) series? In: James, K.H., Lorente, M.A., Pindell, J. (Eds.), Geology of the Area between North and South America, with Focus on the Origin of the Caribbean Plate. vol. 328. Geological Society of London Special Publication, pp. 397–409

Hastie, A.R., Kerr, A.C., 2010. Mantle plume or slab window?: Physical and geochemical constraints on the origin of the Caribbean oceanic plateau. Earth Sci. Rev. 98, 283–293.

Hastie, A.R., Kerr, A.C., Pearce, J.A., Mitchell, S.F., 2007. Classification of altered volcanic island arc rocks using immobile trace elements: development of the Th-Co discrimination diagram. J. Petrol. 48, 2341–2357.

Hastie, A.R., Kerr, A.C., Mitchell, S.F., Miller, I., 2008. Geochemistry and petrogenesis of Cretaceous oceanic plateau lavas in eastern Jamaica. Lithos 101, 323–343.

Hastie, A.R., Kerr, A.C., Mitchell, S.F., Millar, I., 2009. Geochemistry and tectonomagmatic significance of lower Cretaceous island arc lavas from the Devils Racecourse Formation, eastern Jamaica. In: James, K.H., Lorente, M.A., Pindell, J. (Eds.), Geology of the Area between North and South America, with Focus on the Origin of the Caribbean Plate. vol. 328. Geological Society of London Special Publication, pp. 337–359.
Hastie, A.R., Ramsook, R., Mitchell, S.F., Kerr, A.C., Millar, I., Mark, D.F., 2010. Geochemistry of compositionally distinct late Cretaceous back-arc basin lavas: implications for the tectonomagmatic evolution of the Caribbean plate. J. Geol. 118, 655–676.
Hastie, A.R., Mitchell, S.F., Treloar, P.J., Kerr, A.C., Neill, I., Barfod, D.N., 2013. Geochemical components in a Cretaceous island arc: the Th/La-$(Ce/Ce^*)_{Nd}$ diagram and implications for subduction initiation in the inter-American region. Lithos 162-163, 57–69.
Hastie, A.R., Fitton, J.G., Kerr, A.C., McDonald, I., Schwindrofska, A., Hoernle, K., 2016. The composition of mantle plumes and the deep Earth. Earth Planet. Sci. Lett. 444, 13–25.
Hauff, F., Hoernle, K., Tilton, G., Graham, D.W., Kerr, A.C., 2000. Large volume recycling of oceanic lithosphere over short time scales: Geochemical constraints from the Caribbean Large Igneous Province. Earth Planet. Sci. Lett. 174, 247–263.
Hill, I.G., Worden, R.H., Meighan, I.G., 2000. Yttrium: the immobility-mobility transition during basaltic weathering. Geology 28, 923–926.
Jolly, W.T., Lidiak, E.G., 2006. Role of crustal melting in petrogenesis of the Cretaceous Water Island Formation (Virgin Islands, Northeast Antilles Island arc). Geol. Acta 4, 7–33.
Jolly, W.T., Lidiak, E.G., Schelleckens, H.S., Santos, S., 1998a. Volcanism, tectonics, and stratigraphic correlations in Puerto Rico. In: Lidiak, E.G., Larne, D.K. (Eds.), Tectonics and Geochemistry of the Northeast Caribbean. vol. 322. Geological Society of America, Special Papers, pp. 1–34.
Jolly, W.T., Lidiak, E.G., Dickin, A.P., Wu, T.W., 1998b. Geochemical diversity of Mesozoic island arc tectonic blocks in eastern Puerto Rico. In: Lidiak, E.G., Larne, D.K. (Eds.), Tectonics and Geochemistry of the Northeast Caribbean. vol. 322. Geological Society of America, Special Papers, pp. 67–98.
Jolly, W.T., Lidiak, E.G., Dickin, A.P., 2006. Cretaceous to Mid-Eocene pelagic sediment budget in Puerto Rico and the Virgin Islands (Northeast Antilles Island arc). Geol. Acta 4, 35–62.
Jolly, W.T., Lidiak, E.G., Dickin, A.P., 2008. Bimodal volcanism in Northeast Puerto Rico and the Virgin Islands (Greater Antilles Island Arc): Genetic links with Cretaceous subduction of the mid-Atlantic ridge Caribbean spur. Lithos 103, 393–414.
Keppler, H., 1996. Constraints from partitioning experiments on the composition of subduction-zone fluids. Nature 380, 237–240.
Kerr, A.C., 1998. Oceanic plateau formation: a cause of mass extinction and black shale deposition around the Cenomanian-Turonian boundary. J. Geol. Soc. Lond. 155, 619–626.
Kerr, A.C., 2005. Oceanic LIPs: the kiss of death. Elements 1, 289–292.
Kerr, A.C., Iturralde-Vinent, M.A., Saunders, A.D., Babbs, T.L., Tarney, J., 1999. A new plate tectonic model of the Caribbean: implications from a geochemical reconnaissance of Cuban Mesozoic volcanic rocks. Geol. Soc. Am. Bull. 111, 1581–1599.
Kerr, A.C., White, R.V., Thompson, P.M.E., Tarney, J., Saunders, A.D., 2003. No oceanic plateau - no caribbean plate? The seminal role of an oceanic plateau in caribbean plate evolution. In: Bartolini, C., Buffler, R.T., Blickwede, J. (Eds.), The Circum Gulf of Mexico and Caribbean: Hydrocarbon Habitats Basin Formation and Plate Tectonics. vol. 79. American Association of Petroleum Geology Memoir, pp. 126–268.
Kesler, S.E., Campbell, I.H., Allen, C.M., 2005. Age of the Los Ranchos Formation, Dominican Republic: timing and tectonic setting of primitive island arc volcanism in the Caribbean region. Geol. Soc. Am. Bull. 117, 987–995.
Kessel, R., Schmidt, M.W., Ulmer, P., Pettke, T., 2005. Trace element signature of subduction zone fluids, melts and supercritical liquids at 120–180km depth. Nature 437, 724–727.
Kurtz, A.C., Derry, L.A., Chadwick, O.A., Alfano, M.J., 2000. Refractory element mobility in volcanic soils. Geology 28, 683–686.
Lebron, M.C., Perfit, M.R., 1993. Stratigraphic and petrochemical support subduction polarity reversal of the Cretaceous Caribbean Island arc. J. Geol. 101, 389–396.
Lebron, M.C., Perfit, M.R., 1994. Petrochemistry and tectonic significance of Cretaceous island-arc rocks, Cordillera Oriental, Dominican Republic. Tectonophysics 229, 69–100.
Leroy, S., Mauffret, A., 1996. Intraplate deformation in the Caribbean region. J. Geodyn. 21, 113–122.
Lidiak, E.G., Anderson, T.H., 2015. Evolution of the Caribbean plate and origin of the Gulf of Mexico in light of plate motions accommodated by strike-slip faulting. In: Anderson, T.H., Didenko, A.N., Johnson, C.L., Khanchuk, A.I., MacDonald, J.H. (Eds.), Late Jurassic Margin of Laurasia - A Record of Faulting Accommodating Plate Rotation. Geological Society of America Special Paper 513. https://doi.org/10.1130/2015.2513(01).
Mann, P., Calais, E., Ruegg, J.-C., DeMets, C., Jansma, P.E., Mattioli, G.S., 2002. Oblique collision in the northeastern Caribbean from GPS measurements and geological observations. Tectonics 21. https://doi.org/10.1029/2001TC001304.
Mann, P., Rogers, R., Gahagan, L.M., 2007. Overview of plate tectonic history and its unresolved tectonic problems. In: Bundschuh, J., Alvarado, G. (Eds.), Central America. Geology, Resources and Hazards 1. 1. Taylor and Francis, London, pp. 201–237.
Marchesi, C., Garrido, C.J., Bosch, D., Proenza, J.A., Gervilla, F., Monie, P., Rodríguez-Vega, A., 2007. Geochemistry of Cretaceous magmatism in eastern Cuba: recycling of North American continental sediments and implications for subduction polarity reversal in the Greater Antilles paleo-arc. J. Petrol. 48, 1813–1840.
Marchesi, C., Garrido, C.J., Proenza, J.A., Hidas, K., Varas-Reus, M.I., Butjosa, L., Lewis, J.F., 2016. Geochemical record of subduction initiation in the sub-arc mantle: insights from the Loma Caribe peridotite (Dominican Republic). Lithos 252-253, 1–15.
McDonald, I., Viljoen, K.S., 2006. Platinum-group element geochemistry of mantle eclogites: a reconnaissance study of xenoliths from the Orapa kimberlite, Botswana. Appl. Earth Sci. 115, 81–93.
McDonough, W.F., Sun, S.-s., 1995. The composition of the Earth. Chem. Geol. 120, 223–253.
McKenzie, D., O'Nions, 1991. Partial melt distributions from inversion of rare earth element concentrations. J. Petrol. 32, 1021–1091.
Neill, I., Gibbs, J.A., Hastie, A.R., Kerr, A.C., 2010. Origin of the volcanic complexes of La Désirade, Lesser Antilles: Implications for tectonic reconstruction of the Late Jurassic to Cretaceous Pacific-proto Caribbean margin. Lithos 120, 407–420.
Neill, I., Kerr, A.C., Hastie, A.R., Stanek, K.-P., Millar, I.L., 2011. Origin of the Aves Ridge and Dutch-Venezuelan Antilles: interaction of the Cretaceous "Great Arc" and Caribbean-Colombian Oceanic Plateau? J. Geol. Soc. Lond. 168, 333–347.
Neill, I., Kerr, A.C., Chamberlain, K.R., Schmitt, A.K., Urbani, F., Hastie, A.R., Pindell, J.L., Barry, T.L., Millar, I.L., 2014. Vestiges of the proto-Caribbean seaway: origin of the San Souci Volcanic Group, Trinidad. Tectonophysics 626, 170–185.
Nowell, G.M., Kempton, P.D., Noble, S.R., 1998. High precision Hf isotope measurements of MORB and OIB by thermal ionisation mass spectrometry: insights into the depleted mantle. Chem. Geol. 149, 211–233.
Patino, L.C., Velbel, M.A., Price, J.R., Wade, J.A., 2003. Trace element mobility during spheroidal weathering of basalts and andesites in Hawaii and Guatemala. Chem. Geol. 202, 343–364.
Pearce, J.A., Peate, D.W., 1995. Tectonic implications of the composition of volcanic arc magmas. Ann. Rev. Earth Planet. Sci. Lett. 23, 251–285.
Pindell, J.L., Kennan, L., 2009. Tectonic evolution of the Gulf of Mexico, Caribbean and northern South America in the mantle reference frame: an update. In: James, K.H., Lorente, M.A., Pindell, J. (Eds.), Geology of the Area between North and South America, With Focus on the Origin of the Caribbean Plate. vol. 328. Geological Society of London Special Publication, pp. 1–55.
Pindell, J., Kennan, L., Stanek, K.P., Maresh, W.V., Draper, G., 2006. Foundations of Gulf of Mexico and Caribbean evolution: eight controversies resolved. Geol. Acta 4, 303–341.
Pindell, J., Maresch, W.V., Martens, U., Stanek, K., 2011. The Greater Antillean Arc: Early Cretaceous origin and proposed relationship to Central American subduction mélanges: implications for models of Caribbean evolution. Int.Geol. Rev. 54, 1–13.
Plank, T., 2014. The chemical composition of subducting sediments. Treatise on Geochemistry, second edition Elsevier, pp. 607–629.
Rankin, D., 2002. Geology of St. John, U.S. Virgin Islands. United States Geological Survey Professional Paper. 1631 pp. 1–36.
Schelleckens, J.H., 1998. Geochemical evolution and tectonic history of Puerto Rico. In: Lidiak, E.G., Larne, D.K. (Eds.), Tectonics and Geochemistry of the Northeast Caribbean. Geological Society of America, Special Papers vol. 322, pp. 35–66.
Shaw, D.M., 1970. Trace element fractionation during anatexis. Geochim. Cosmochim. Acta 34, 237–243.
Smith, A.L., Schellekens, J.H., Muriel Díaz, A.-L., 1998. Batholiths as markers of tectonic change in the northeastern Caribbean. In: Lidiak, E.G., Larue, D.K. (Eds.), Tectonics and Geochemistry of the Northeastern Caribbean: Boulder, Colorado. Geological Society of America Special Paper vol. 322, pp. 99–122.
Spikings, R., Cochrane, R., Villagomez, D., Van der Lelij, R., Vallejo, C., Winkler, W., Beate, B., 2015. The geological history of northwestern South America: from Pangaea to the early collision of the Caribbean Large Igneous Province (290-75 Ma). Gondw. Res. 27, 95–139.
Sun, S.-s., McDonough, W.F., 1989. Chemical and isotope systematics of oceanic basalts: implications for mantle composition and processes. Magmatism in the Ocean Basins. Geol. Soc. Lond. Spec. Publ. 42, 313–345.
Thompson, P.M.E., Kempton, P.D., White, R.V., Kerr, A.C., Tarney, J., Saunders, A.D., Fitton, J.G., 2003. Hf-Nd isotope constraints on the origin of the Cretaceous Caribbean plateau and its relationship to the Galapagos plume. Earth Planet. Sci. Lett. 217, 59–75.
Torró, L., Garcia-Casco, A., Proenza, J.A., Blanco-Quintero, I.F., Gutiérrez-Alonso, G., Lewis, J.F., 2016. High-pressure greenschist to blueschist facies transition in the Maimón Formation (Dominican Republic) suggests mid-Cretaceous subduction of the Early Cretaceous Caribbean arc. Lithos 266-267, 309–331.
Torró, L., Proenza, J.A., Marchesi, C., Garcia-Casco, A., Lewis, J.F., 2017. Petrogenesis of meta-volcanic rocks from the Maimón Formation (Dominican Republic): Geochemical record of the nascent Greater Antilles paleo-arc. Lithos 278-281, 255–273.
Vallejo, C., Spikings, R.A., Luzieux, L., Winkler, W., Chew, D., Page, L., 2006. The early interaction between the Caribbean Plateau and the NW South American Plate. Terra Nova 18, 264–269.
Vervoort, J.D., Plank, T., Prytulak, J., 2011. The Hf-Nd isotopic composition of marine sediments. Geochim. Cosmochim. Acta 75, 5903–5926.
Woodhead, J.D., 1988. The origin of geochemical variations in Mariana lavas: a general model for petrogenesis in intra-oceanic island arcs? J. Petrol. 29, 805–830.
Wright, J.E., Wyld, S.J., 2011. Late Cretaceous subduction initiation on the eastern margin of the Caribbean-Colombian Oceanic Plateau: one Great Arc of the Caribbean (?). Geosphere 7, 1–26.
Xu, X., Keller, G.R., Guo, X., 2016. Dip variations of the North American and North Caribbean Plates dominate the tectonic activity of Puerto Rico-Virgin Islands and adjacent areas. Geol. J. 51, 901–914.